



# A P/N/S-containing high-efficiency flame retardant endowing epoxy resin with excellent flame retardance, mechanical properties and heat resistance

Jiahao Zou<sup>a</sup>, Huajun Duan<sup>a,b,\*</sup>, Yongsheng Chen<sup>a</sup>, Sa Ji<sup>a</sup>, Jianfan Cao<sup>a</sup>, Huiru Ma<sup>c</sup>

<sup>a</sup> School of Materials Science and Engineering, Wuhan University of Technology, Wuhan, 430070, China

<sup>b</sup> Institute of Advanced Material Manufacturing Equipment and Technology, Wuhan University of Technology, Wuhan, 430070, China

<sup>c</sup> Department of Chemistry, School of Chemistry, Chemical Engineering and Life Science, Wuhan University of Technology, Wuhan, 430070, China

## ARTICLE INFO

### Keywords:

Epoxy resin  
High efficiency  
Flame retardance  
Heat resistance  
Mechanical properties

## ABSTRACT

In order to improve the flame retardancy while maintaining the excellent mechanical properties and heat resistance of epoxy resin, a novel P/N/S-containing high efficiency flame retardant named TAP was designed and synthesized by a simple one-pot reaction among 2-thenaldehyde, 2-aminobenzothiazole (ABZ) and 9,10-dihydro-9-oxa-10-phosphaphenanthrene-10-oxide (DOPO). The chemical structure of TAP was characterized by Fourier transform infrared (FTIR) spectroscopy, <sup>1</sup>H and <sup>31</sup>P nuclear magnetic resonance (NMR) spectroscopy. Compared to pure EP, the introduction of TAP can reduce the thermal decomposition rate of epoxy resin and increase the char residue. Meantime, when the phosphorus content was only 0.48%, EP/7.5%TAP passed the vertical burning V-0 rating, obtaining a high flame-retardant efficiency. With the addition of 10 wt% TAP, the limiting oxygen index (LOI) value increased from 22.8% of pure EP to 31.5%, while the peak heat release rate (PHRR), total heat release (THR) and total smoke production (TSP) values decreased by 41.26%, 35.70% and 24.03%, respectively. In addition, the glass transition temperature (*T<sub>g</sub>*) of the epoxy resin decreased from 185 °C to 177 °C, while the storage modulus at 30 °C increased. Subsequently, the flexural tests of the samples revealed that the mechanical properties were well maintained. All these results demonstrated that the TAP was a novel high efficiency flame retardant for EP, which enabled the cured EP to maintain excellent heat resistance and mechanical properties.

## 1. Introduction

As an important part of the common thermosetting resin system, epoxy resin is used in fields of industry and life because of its excellent chemical corrosion resistance, good insulation for electricity, strong bonding strength and better mechanical properties than ordinary thermosetting materials [1–4]. Due to these remarkable advantages, epoxy resin is selected for application in a variety of environments. However, one of the major factors restricting the use of epoxy resin in practical applications is its high flammability, which is also an influencing factor that must be considered in the practical use of most polymeric materials [5]. In view of the poor flame resistance of the resin matrix, much work has been done to improve the flame resistance [6–9]. For example, Yu B et al. [10] prepared hydroxylated hexagonal boron nitride (BNO) and it was covalently bonded with (3-isocyanate propyl) triethoxysilane modified epoxy resin. Adding 3 wt% BNO caused *T<sub>g</sub>* of EP nanocomposites to increase by 42.7 °C. The PHRR and THR of EP nanocomposites were reduced by 53.1% and 32.6%, while the release of toxic fumes was suppressed. More recently, Howell B A et al. [11] treated

deoxyanisodamine with DOPO to obtain an intermediate product, then the intermediate product was converted into the corresponding bisphenol compound (BDE), which was used as flame retardant hardener for epoxy resin. The results indicated that epoxy resin cured by BDE achieved UL-94 V-0 rating, and the limited oxygen index (LOI) value increased from 18.8% to 35.6%.

Introducing flame retardant components into the resin matrix is one of the most direct and effective methods, such as the synthesis of monomers with flame retardant function and the addition of various flame retardants. The method of adding flame retardants has been partially industrialized because of its strong operability. Simultaneously, it has advantages in functionalizing materials, so it has been widely studied and discussed [12].

Due to the low cost, high efficiency and having small impact on the mechanical properties of the matrix, halogen-containing flame retardants were the focus of the initial research [13,14]. Halogen-containing flame retardants, especially bromine-containing flame retardants, are mainly based on the gas-phase flame retardant effect [15]. The halogen-containing flame retardant will release a series

\* Corresponding author. School of Materials Science and Engineering, Wuhan University of Technology, Wuhan, 430070, China.

E-mail address: [dhj@whut.edu.cn](mailto:dhj@whut.edu.cn) (H. Duan).

<https://doi.org/10.1016/j.compositesb.2020.108228>

Received 4 April 2020; Received in revised form 11 June 2020; Accepted 14 June 2020

Available online 21 July 2020

1359-8368/© 2020 Elsevier Ltd. All rights reserved.

of halogenated hydrogen during the combustion process, which can capture the active radicals generated during combustion. As a result, the chain reaction of combustion is terminated, thereby protecting the material from further combustion.

However, with the increasing emphasis on environmental protection issues, the disadvantages of halogen-containing flame retardants have been deeply recognized [11]. The organohalogen compounds can be converted into toxic dioxins at high temperatures [16]. At the same time, these toxic and harmful substances cannot be biodegraded, which will cause them to be exposed to the environment and accumulate in the organism, causing great harm to the environment and health [17–19]. Therefore, in order to meet the requirements of environmental protection, the importance of related research on halogen-free flame retardants has been highlighted.

In recent years, the research on 9,10-dihydro-9-oxa-10-phosphaphenanthrene-10-oxide (DOPO) is the most prominent in the research of halogen-free flame retardants for epoxy resin, due to that the special phosphaphenanthrene structure of DOPO endows epoxy resin with good heat resistance and flame retardancy. Meanwhile, the active P–H bond in the molecule can participate in the reaction to obtain derivatives containing different functional groups [20–24].

However, a single DOPO based flame retardant which only contains phosphorus element requires substantial addition to ensure excellent flame retardancy. Therefore, other elements have been introduced into the molecular structure of phosphorus compounds in an effort to enhance flame-retarding properties including nitrogen [25,26], sulfur [27,28], silicon [29,30], boron [31,32]. Fortunately, DOPO and related derivatives have a satisfactory mutual promotion effect with other elements, which reduce the amount of flame retardant additives under the premise of ensuring flame-retardant properties.

Sulfur-containing compounds are an important component used to improve flame retardant efficiency, especially sulfur-containing heterocyclic compounds, which has good flame-retardant effect in condensed phase and gas phase. Xu M et al. [33] reported a novel phosphorus and sulfur-containing epoxy resin curing agent (ABTPPO), which contains thiophene ring and phosphine oxide structure. The results proved that ABTPPO can further degrade to form phosphoric acid and sulfuric acid during combustion, which can promote the dehydration and carbonization of the matrix to form a protective carbon layer and improve the flame retardancy of the epoxy resin. Cheng J et al. [34] synthesized an aminobenzothiazole-substituted cyclotriphosphazene derivative (ABCP). It is worth noting that the phenomenon of sulfur and

phosphorus catalyzed carbon formation was also observed after ABCP was used in epoxy resins. Wang P et al. [35] synthesized a series of flame retardants for epoxy resins based on DOPO and thiazole derivatives. The results showed that thiazole derivatives can produce non-combustible sulfur-containing gas and ammonia during combustion and exerted a satisfactory flame-retardant effect in the gas phase.

In most cases, however, the addition of flame retardants brings excellent flame retardancy effects while adversely affecting other properties, such as the sharp deterioration of mechanical properties and the decline in heat resistance, which will limit the scope of application of materials. Considering the above situation, it is of great importance to synthesize an efficient flame retardant for epoxy resin to enhance the flame retardancy while maintaining the excellent mechanical properties and heat resistance of epoxy resin.

Therefore, for this work, two heterocyclic compounds containing nitrogen and sulfur were selected to work with DOPO to synthesize the P/N/S ternary flame retardant TAP in a facile one-pot process. A series of samples with different amounts of flame retardant were prepared by using 4,4'-diaminodiphenylsulfone (DDS) as epoxy curing agent. The thermal stability, flame retardancy and combustion behavior of samples were investigated using TGA, LOI, UL-94 and cone calorimetry tests (CCT). And the flame-retardant mechanism was discussed in detail through various measurements. Besides, the heat resistance and mechanical properties of samples were also studied.

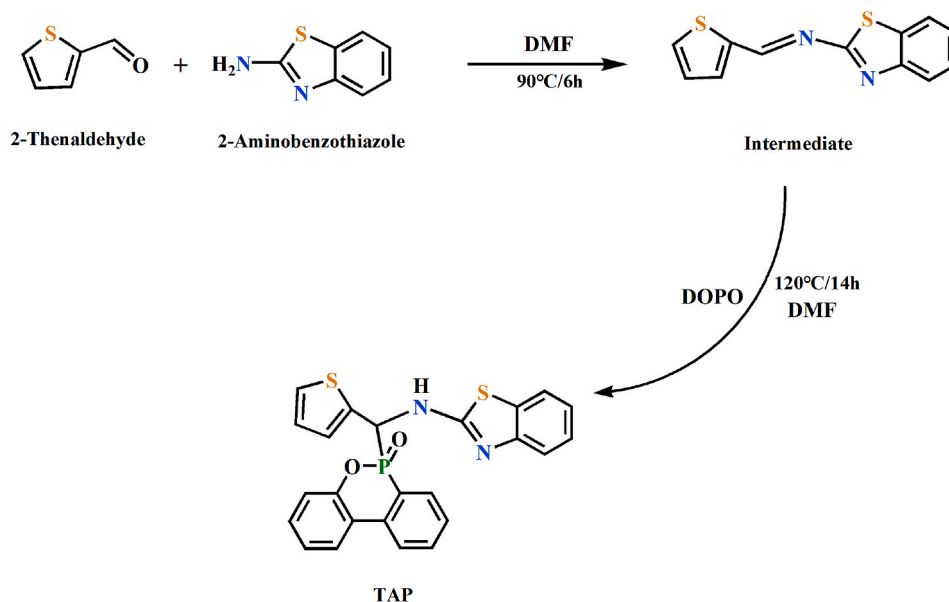
## 2. Experimental section

### 2.1. Materials

2-aminobenzothiazole (ABZ) was purchased from Aladdin Industrial Co., Ltd. 2-Thenaldehyde was obtained from Shanghai MackLin Biochemical Co., Ltd. DOPO was provided by Huizhou Shengshi Technology Co., Ltd. N,N-Dimethylformamide (DMF) and methanol were supplied by Sinopharm Chemical Reagent Co., Ltd. Epoxy resin (E-51, the epoxy value of 0.51 mol/100 g) was purchased from Yueyang Baling Huaxing Petrochemical Co., Ltd. DDS was provided by Guangdong Wengjiang Chemical Reagent Co., Ltd.

### 2.2. Synthesis of TAP

15.0 g (0.1 mol) ABZ was dissolved in 100 mL of DMF in a three-necked round-bottomed flask equipped with a reflux condenser and a



Scheme 1. Synthesis route of TAP.

magnetic stirrer. Subsequently, 11.2 g (0.1 mol) 2-thenaldehyde was added and stirred at 90 °C for 6 h. After that, 21.6 g (0.1 mol) DOPO was added to the solution. The reaction mixture was heated to 120 °C and kept at this temperature for 14 h with constant stirring. After the reaction finished, DMF was completely removed by reduced pressure distillation at 120 °C. The crude product was washed three times with excessive methanol and deionized water respectively, and then dried in a vacuum oven at 70 °C for 24 h to obtain off-white powder product (TAP, yield: 62%). The synthesis route of TAP was shown in Scheme 1.

### 2.3. Preparation of curing samples

EP curing samples with different proportions of TAP and pure EP curing sample were prepared as follows. After EP was heated to 180 °C, the powdery TAP was added and the mixture was stirred constantly until TAP was completely dissolved in EP to obtain a transparent liquid. The curing agent DDS was added when the uniform transparent liquid was cooled to 120 °C. Subsequently, the mixture was further stirred until a homogeneous solution was obtained. Finally, the solution was poured rapidly into a preheated metal mold and cured at 150 °C for 3 h, 180 °C for 3 h and 210 °C for 2 h.

The pure EP thermosets were prepared by the same procedure without the addition of TAP. Besides, the samples were labeled according to the mass fraction of flame retardant in epoxy thermosets. The detailed formulas are listed in Table 1.

### 2.4. Characterizations

Fourier transform infrared (FTIR) spectra were performed on a Nicolet 6700 infrared spectrometer (Nicolet, America). The synthesized product was tested using KBr tablet method in the wavenumber of 4000 to 400  $\text{cm}^{-1}$ .

$^1\text{H}$  and  $^{13}\text{P}$  nuclear magnetic resonance (NMR) spectroscopy were recorded on a Bruker AV400 NMR spectrometer (Bruker, Switzerland). Deuterated dimethyl sulfoxide ( $\text{DMSO}-d_6$ ) was adopted as the test solvent.

Thermogravimetric analysis (TGA) was operated on STA449F3 (NETZSCH, Germany) under a nitrogen atmosphere. The temperature was increased from room temperature to 800 °C at a heating rate of 10 °C/min.

The limited oxygen index (LOI) values were measured according to ASTM D2863 using a JF-3 oxygen index meter (Jiang Ning, China). The size of the tested samples was  $100 \times 6.5 \times 3 \text{ mm}^3$ .

The vertical burning (UL-94) ratings were tested on a NK8017A instrument (Nklsky, China) according to ASTM D3801 standard. The dimension of all the specimens was  $130 \times 13 \times 3 \text{ mm}^3$ .

The combustion behavior of the thermosetting material was analyzed using an FTT0007 cone calorimeter (FTT, UK) in accordance with ISO 5660. The sample with the size of  $100 \times 100 \times 3 \text{ mm}^3$  was tested with a heat radiation value of 50  $\text{kW/m}^2$ .

Dynamic mechanical analysis (DMA) was conducted on a PerkinElmer DMA8000 (PE, USA) at a heating rate of 5 °C/min in a temperature range from room temperature to 250 °C. The test region of the three-point bending test was  $40 \times 6 \times 3 \text{ mm}^3$ .

The morphology of char residue of EP thermoset after CCT was

**Table 1**  
Formulations of cured epoxy.

Sample	E-51 (g)	DDS (g)	TAP (g)	Content of TAP (wt %)	Content of Phosphorus (wt%)
EP	100	31.60	0	0	0
EP/7.5%TAP	100	31.60	10.67	7.50	0.48
EP/10%TAP	100	31.60	14.62	10.00	0.67
EP/12.5%TAP	100	31.60	18.80	12.50	0.84

observed using a TESCAN VEGA3 (Czech Republic) scanning electron microscopy (SEM).

Laser raman spectroscopy (LRS) test was carried out on an InVia laser raman spectrometer (RENISHAW, Britain) with an excitation wavelength of 633 nm and a scanning range of 800–2000  $\text{cm}^{-1}$  to further investigate the carbon residue.

Pyrolysis-gas chromatography/mass spectrometry (Py-GC/MS) was performed under helium (He) atmosphere by using an Agilent 7890/5975 GC/MS (Agilent, USA). The injector temperature was increased from 50 °C to 280 °C at a heating rate of 10 °C/min, and the pyrolysis temperature was 500 °C.

The universal material testing machine (Instron 5967, USA) was used to test the flexural properties of the samples. Three-point bending test was conducted with a constant rate of 1 mm/min according to ASTM D790, and five specimens were measured for each sample.

## 3. Results and discussion

### 3.1. Characterization of TAP

The FTIR spectra of DOPO, ABZ and TAP were presented in Fig. 1. It was observed that the peaks at 3396  $\text{cm}^{-1}$  and 3271  $\text{cm}^{-1}$  were ascribed to  $-\text{NH}_2$  of ABZ. Correspondingly, in the FTIR spectra of TAP, there was characteristic peak at 3226  $\text{cm}^{-1}$  belonging to N–H bond. The peak at around 3014  $\text{cm}^{-1}$  was ascribed to the vibration of aromatic-H; the absorption peak at 1531  $\text{cm}^{-1}$  was attributed to benzene ring; the absorption peak at 1448  $\text{cm}^{-1}$  belonged to C=N bond in the thiazole ring; the absorption peaks were found at 1235  $\text{cm}^{-1}$ , 936  $\text{cm}^{-1}$  and 755  $\text{cm}^{-1}$  corresponding to P=O, P–O–Ph and P–C [36], confirming the existence of the phosphaphenanthrene. Meanwhile, the peak of P–H at 2437  $\text{cm}^{-1}$  disappeared in the FTIR spectrum of TAP [37], which indicated that the addition reaction between intermediate and DOPO had occurred.

The  $^1\text{H}$  NMR and  $^{31}\text{P}$  NMR spectra were applied to further demonstrate the structure of TAP which were shown in Fig. 2. The chemical shifts at 7.0–8.2 ppm belonged to aromatic-H of heterocyclic ring and benzene ring. It was found that there were two shifts at 6.01 and 6.24 ppm attributed to the hydrogen atom on a chiral carbon which was linked with DOPO group. It's interesting to note that the chemical shift of N–H also had two signals at 9.10 and 9.22 ppm. This phenomenon was caused by the existence of a special kind of chiral atoms in the TAP molecular structure. Because of the presence of chiral atoms, the difference of stereochemical structures of the compound produced different chemical shifts, which led to the emergence of two groups of signals [38,39]. Moreover, the integral area ratio of N–H, C $^*$ -H and

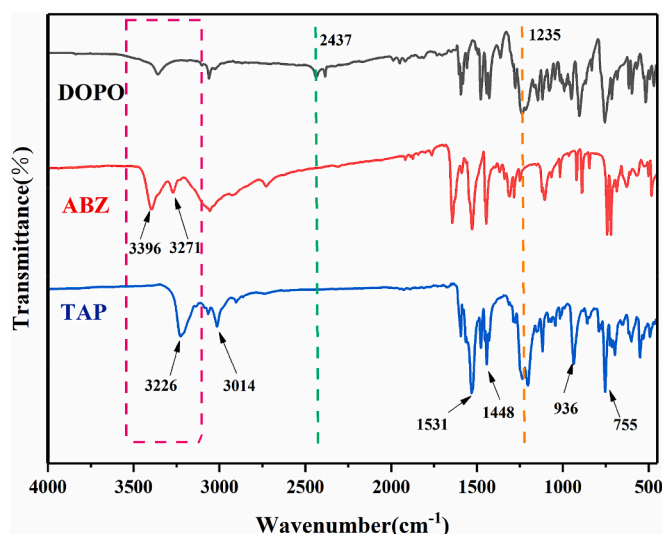


**Fig. 1.** FTIR spectra of DOPO, ABZ and TAP.

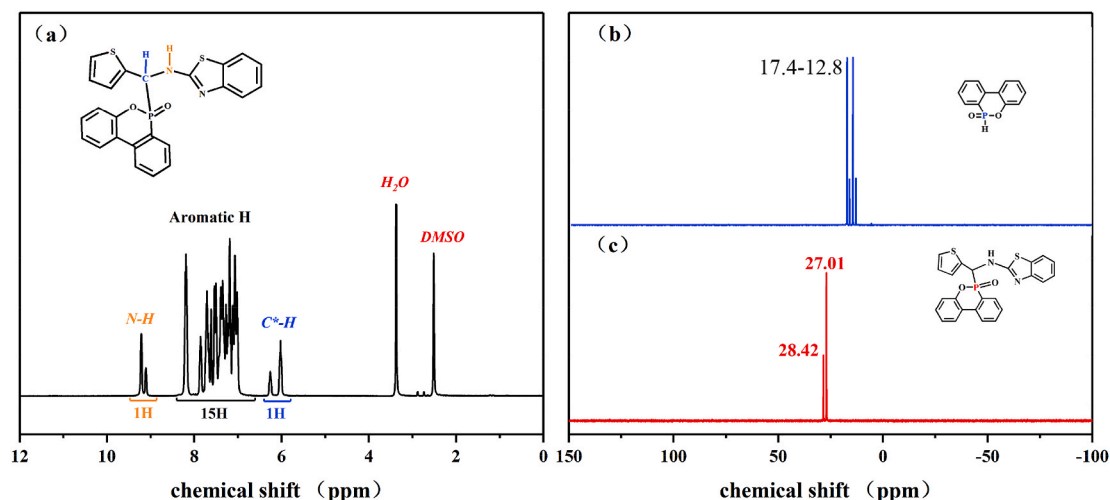


Fig. 2.  $^1\text{H}$  NMR spectra of TAP (a) and  $^{31}\text{P}$  NMR spectra of DOPO (b) and TAP (c).

aromatic-H is about 1:1:15, which corresponds to the theoretical value. Furthermore, two signals at 27.01 and 28.42 ppm also appeared in the  $^{31}\text{P}$  NMR spectra of TAP, which was consistent with the phenomenon mentioned above, while the chemical shift of phosphorus atom in DOPO shown in Fig. 2(b) was at 17.4–12.8 ppm. The above characterization methods indicated that target product TAP was successfully synthesized.

### 3.2. Thermal stability of modified samples

The TG and DTG curves, which was used to evaluate thermal stability of thermosetting resin and TAP under  $\text{N}_2$  atmosphere, were shown in Fig. 3. The relevant data can be seen in Table 2, including the initial decomposition temperature ( $T_{5\%}$ ), the maximum weight loss temperature ( $T_{\text{max}}$ ), the maximum mass loss rate ( $\text{MLR}_{\text{max}}$ ), as well as the char residue at 800  $^\circ\text{C}$ .

As shown in Fig. 3 and Table 2, the  $T_{5\%}$  of the flame retardant was 304  $^\circ\text{C}$ , which was lower than 389  $^\circ\text{C}$  of pure epoxy, proving the degradation of flame retardant occurred before the degradation of pure epoxy. It was the reason why the degradation temperature of modified EP decreased. Besides, TAP showed two main decomposition processes in the pyrolysis process, the first stage was at 275–354  $^\circ\text{C}$  with a peak value of 316  $^\circ\text{C}$ , corresponding to the breakage of some weak bonds,

Table 2

Thermogravimetric data of epoxy thermosets and TAP.

Sample	$T_{5\%}$ ( $^\circ\text{C}$ )	$T_{\text{max}}$ ( $^\circ\text{C}$ )	$\text{MLR}_{\text{max}}$ (%/min)	Char residue (wt%)
EP	389	419	20.10	15.49
EP/7.5%TAP	348	400	15.73	18.65
EP/10%TAP	340	394	14.42	19.23
EP/12.5%TAP	336	388	13.72	18.31
TAP	304	316, 455	7.57, 5.61	15.47

such as P–O–C and P–C [40]. The peak value of the second stage was 455  $^\circ\text{C}$ , and the temperature span of this stage was larger than that of the first stage, which involved the degradation of various aromatic rings and the release of all kinds of gases. This issue will be discussed in more detail in the following sections. Moreover, at a high temperature of 800  $^\circ\text{C}$ , TAP remained 15.47% residue.

As for modified thermosetting samples, their DTG and TG curves indicated a typical one-step degradation model in nitrogen. The  $T_{5\%}$  of EP gradually decreased from 389  $^\circ\text{C}$  to 336  $^\circ\text{C}$  due to the advance degradation of TAP. The same trend also occurred at the value of  $T_{\text{max}}$ ,

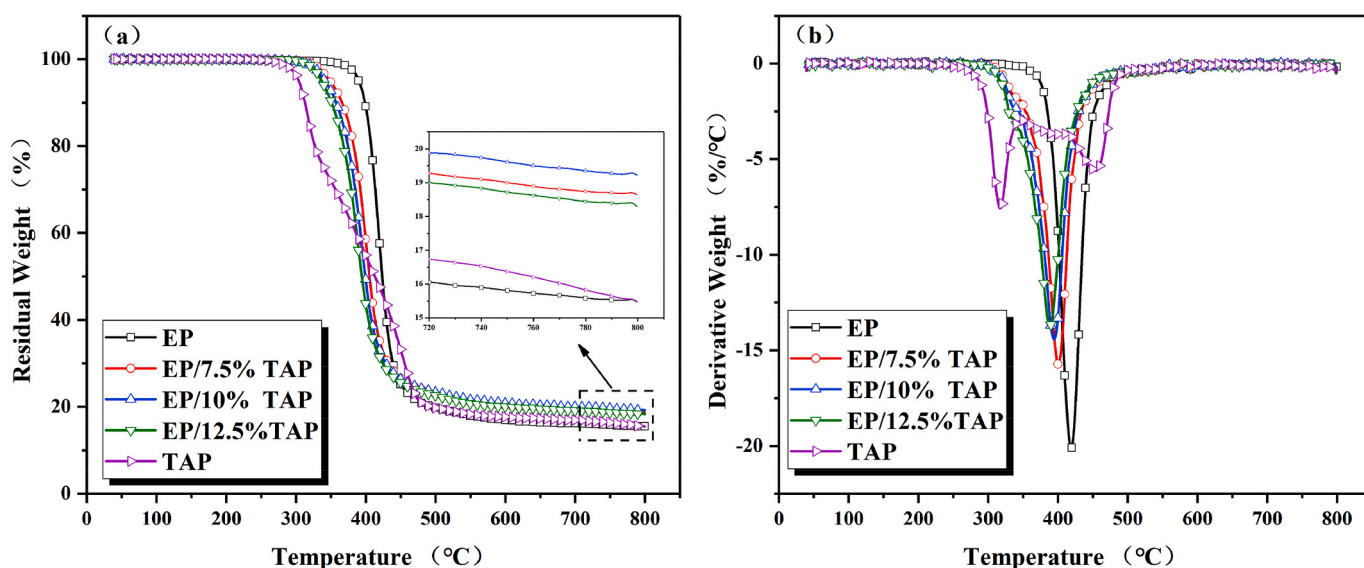


Fig. 3. TG (a) and DTG (b) curves of epoxy thermosets under nitrogen atmosphere.

which decreased from 419 °C to 388 °C, showing a slight decline. Fortunately, the maximum weight-loss rate dropped significantly from 20.10%/min to 13.72%/min, which proved that the addition of TAP can improve the thermal stability of thermosetting resin by prolonging the decomposition process of resin matrix. The char residue of pure EP was almost the same as that of TAP at high temperature, which was 15.49%. Obviously, with the increasing amount of TAP, the char residue at 800 °C also increased, which gave an evidence to that epoxy resins added with flame retardant exhibit more efficient capacity of carbonization. In a word, based on TGA of the samples, the products generated from early degradation of TAP led to the degradation of the matrix in advance. With the degradation of TAP, a series of complex byproducts generated by the degradation of DOPO group and heterocyclic ring will be produced at higher temperatures, which induced the decrease of MLR<sub>max</sub> of the matrix and the increase of the final char residue.

### 3.3. Flame retardance and combustion behavior of modified samples

LOI and UL-94 tests were used to evaluate the flame retardance of the cured epoxy resins. The data were listed in Table 3. The pure EP had poor flame retardancy with LOI value of 22.8% and failed to pass UL-94 test. However, with the increasing amount of TAP, the unfavorable situation changed. With 7.5 wt% amount of TAP in EP, the LOI value increased from 22.8% to 30.8%. Moreover, when the phosphorus content was only 0.48%, EP/7.5%TAP sample passed a vertical UL-94 V-0 rating, indicating excellent flame-retardant efficiency. Increasing the mass fraction of TAP, a higher LOI value and UL-94 V-0 rating was obtained. The LOI value of EP/10%TAP increased to 31.5%, which was 38% higher than that of pure epoxy. The slightly drop of LOI value in EP/12.5%TAP was due to the release of excess gases, which caused the destruction of the carbon layer. It can be concluded from the data that TAP is a highly effective flame retardant, which can bring excellent flame retardance to epoxy resin at low phosphorus content.

CCT is one of the most effective way to estimate the combustion behaviors of the polymeric materials [41,42]. By this means a set of specific parameters about the flammability of materials can be obtained, including the time to ignition (TTI), peak heat release rate (PHRR), total heat release (THR), total smoke production (TSP), average effective heat combustion (av-EHC), fire growth rate index (FIGRA), average CO yield (av-COY), average CO<sub>2</sub> yield (av-CO<sub>2</sub>Y) and char residue after the combustion.

It was obviously that the TTI of the pure EP was 73 s while samples with flame retardant were significantly shortened to around 64 s. During the early heating process of the material, the degradation of the TAP will catalyze the further degradation of the matrix, resulting in the weaker resistance of EP matrix to ignition.

The HRR is a critical parameter that characterize the intensity of combustion. As shown in Table 4, pure EP had the maximum combustion intensity with a PHRR of 1141.50 kW/m<sup>2</sup> in several groups of samples. Compared with the high PHRR of pure EP, the values of other flame-retardant samples were greatly reduced. EP/10%TAP had the lowest combustion intensity with a PHRR of 670.41 kW/m<sup>2</sup>, standing for a 41.26% reduction. Meanwhile, the THR of flame-retardant samples sharply reduced from 81.53 MJ/m<sup>2</sup> of pure EP to 52.42 MJ/m<sup>2</sup> of EP/10%TAP, demonstrating that the introduction of TAP suppressed the heat release in the combustion process of polymeric materials. However, with the increase of the gas pressure in the carbon layer caused by the

**Table 3**  
Flammability test results of epoxy thermosets.

Sample	LOI (%)	UL-94	Dripping
EP	22.8	No Rating	YES
EP/7.5%TAP	30.8	V-0	NO
EP/10%TAP	31.5	V-0	NO
EP/12.5%TAP	31.3	V-0	NO

**Table 4**  
Cone calorimetric test results of epoxy thermosets.

Sample	EP	EP/7.5%TAP	EP/10%TAP	EP/12.5%TAP
TTI (s)	73	64	66	62
PHRR (kW/m <sup>2</sup> )	1141.50	857.93	670.41	753.71
THR (MJ/m <sup>2</sup> )	81.53	59.09	52.42	53.93
av-EHC (MJ/kg)	21.77	17.58	15.92	16.11
TSP (m <sup>2</sup> )	17.20	13.23	13.11	13.54
FIGRA (kW/(m <sup>2</sup> . s))	7.98	6.04	4.89	5.38
COY (kg/kg)	0.0683	0.0883	0.0879	0.0900
CO <sub>2</sub> Y (kg/kg)	1.87	1.44	1.30	1.31
Char residue (wt%)	5.12	18.85	21.14	20.05

release of the excess gas, the carbon layer was further destroyed at high temperature. Therefore, the flame-retardant effect decreased when the amount of flame retardant reaches 12.5%, manifesting as a decrease of THR and PHRR values.

Furthermore, FIGRA, which is equal to the ratio of PHRR to the time to PHRR, was used to assess the spread rate of fire during combustion. A reduction of FIGRA was seen in flame-retardant samples in Table 4, which mean the fire safety of the thermoset resin had been improved.

EHC is defined as the ratio of HRR to mass loss rate and the magnitude of this parameter reveals the extent to which volatile gases burn during combustion [43]. In Table 4, for the flame-retardant samples, the value of av-EHC followed the same downward trend as well as THR and PHRR. The av-EHC of EP/10%TAP sample was decreased by 26.87%, showing the presence of a gas phase flame-retardant effect. The reason for this phenomenon is believed to be that the introduction of TAP produced some non-flammable gas during combustion, resulting in a dilution effect and the decrease in combustion efficiency. Similarly, a lower av-CO<sub>2</sub>Y and a higher av-COY were seen in Table 4, implying more incomplete combustion occurred during combustion, provided strong evidence for this explanation.

The smoke production capacity of the material is one of the important indexes to evaluate the fire risk. In addition to the serious injury caused by heat release, the respiratory tract injury caused by the smoke in the actual fire site is more fatal [44]. By means of Table 4 and Fig. 4 (c), it can be seen that TAP can also effectively reduce the smoke release of the epoxy, the TSP of EP/10%TAP was reduced by 23.78% from 17.2 to 13.11 m<sup>2</sup> compared to that of pure EP. Based on the above data, it is not difficult to see that the addition of TAP can significantly enhance the flame retardance of epoxy resin while endowing the samples good smoke suppression effect.

Subsequently, Fig. 4(d) showed the variation curve of mass loss with time for several groups of samples. The mass loss rate of pure EP samples was the fastest, and the char residue was the lowest, which was 5.12%. After the addition of flame retardant, the char residue of EP/10%TAP samples was the highest, and the char residue increased to 21.14%, exhibiting a significant increase. Obviously, in the early stage of combustion, the mass loss curve of flame-retardant samples showed a downward trend earlier than that of pure EP, indicating that the flame-retardant samples decomposed in advance under heating conditions, which was consistent with the TGA. It's worth noting that the char residue increased significantly at high temperature, proving that the flame retardant not only works well in the gas phase but also has a good effect in the condensed phase.

In brief, the reason for the results is that TAP containing DOPO groups and sulfur-containing heterocyclic structure prompted formation of char layer in the condensed phase which can hinder the diffusion of combustible volatiles into flame zone and reduce the transmission efficiency of energy and fuel [33,34]. At the same time, some noncombustible gases and phosphorous radical can be released in the combustion process, causing the dilution of combustible gases and the termination of radical chain reaction.

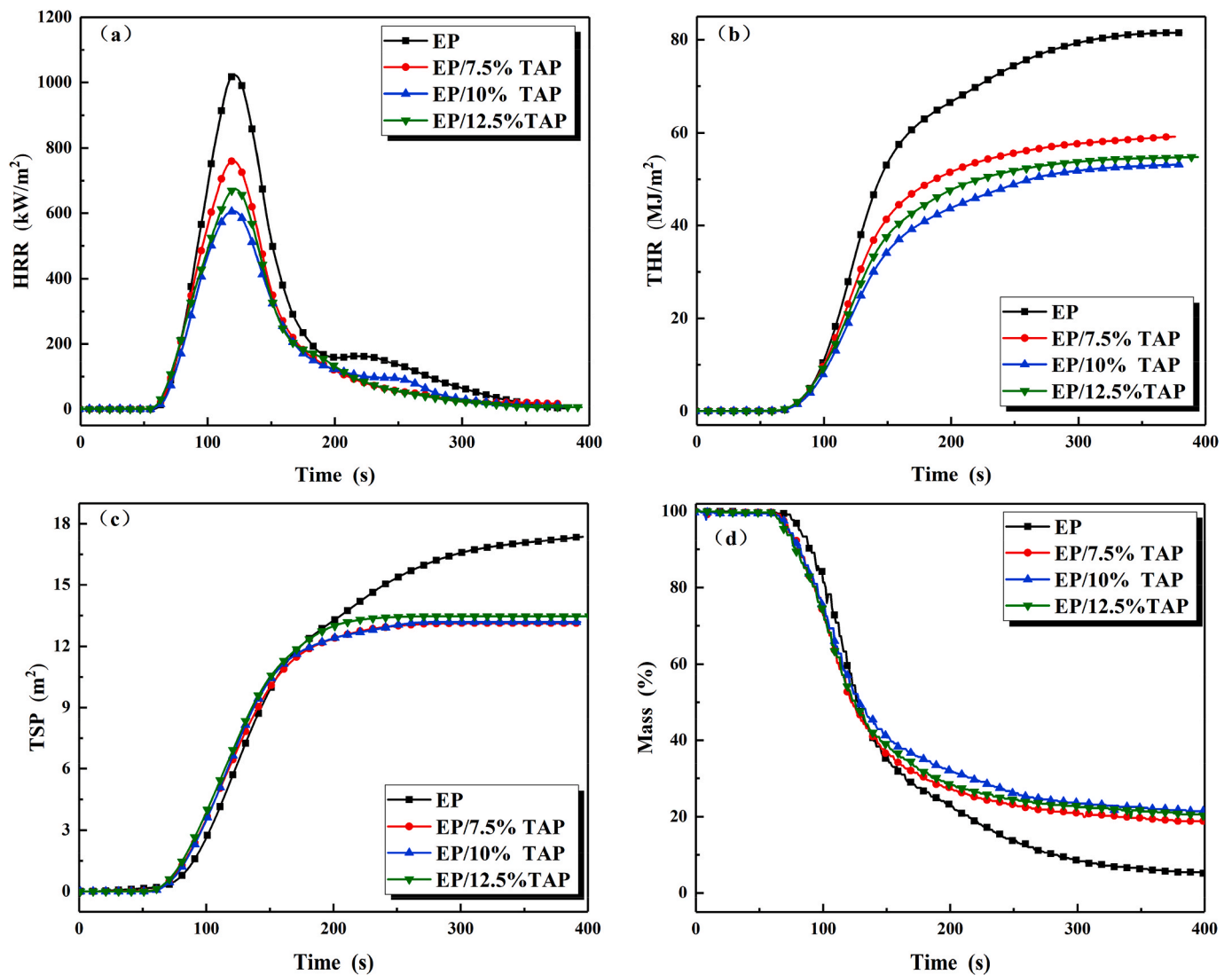


Fig. 4. HRR (a), THR (b), TSP (c) and mass loss(d) curves of epoxy thermosets obtained from cone calorimetry.

### 3.4. Analysis on char residue

During the combustion of polymers, the morphology and structure of the char residue are important indicators for evaluating the flame retardancy. The digital pictures of char residues after cone calorimeter tests for all the samples were displayed in Fig. 5.

As presented in Fig. 5, the residual carbon of the pure EP was cracked without a complete morphology and there were few amounts of residue, which was consistent with the above datum in Table 4. With the increase of TAP content, samples containing TAP had more char residue and showed a more expansive and complete morphology. It was found that there were complex pore structures in the intact expanded carbon layer,

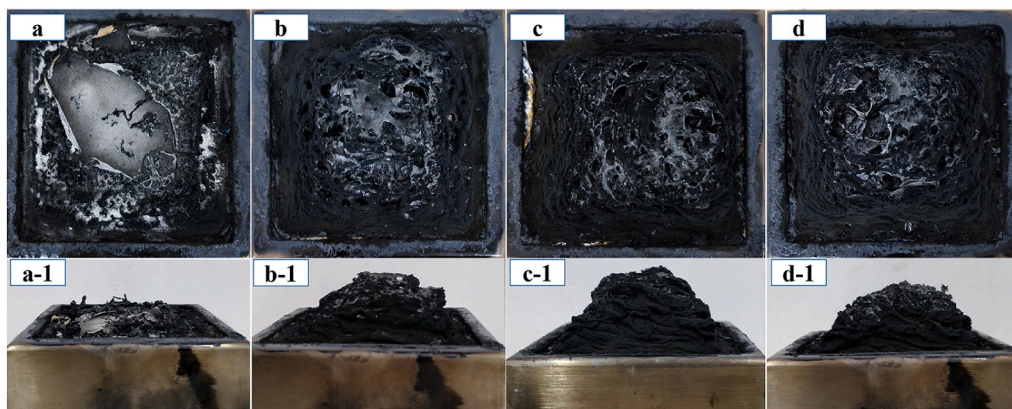


Fig. 5. Digital photos of the char residues of EP (a, a-1), EP/7.5%TAP (b, b-1), EP/10%TAP (c, c-1) and EP/12.5%TAP (d, d-1) after cone calorimeter tests.

which is caused by the release of a large amount of gases produced during combustion. This macroscopic structure is conducive to exerting the shielding effect and dilution effect, while hindering energy and oxygen exchange.

In order to better understand the flame-retardant mechanism in the condensed phase, SEM, Raman spectroscopy and FTIR were used to characterize the microstructure of char residue, and the test results were shown in Fig. 6, Fig. 7 and Fig. 8, respectively. As the macro morphology shown in the digital photos, a broken, perforated and furrowed surface can be clearly observed in the SEM images of pure EP in Fig. 6. With the addition of TAP, the surface of the residue became dense and intact, which can play an important role in preventing the inner matrix from further combustion. Meanwhile, some bubbles were observed on the surface of the char residue. These prominent bubbles were caused by the pyrolysis gas released from the combustion matrix and the degradation of TAP. However, when the dosage of TAP reached 12.5%, excess gas products were generated, which was stored in the internal structure. As the combustion continued, the internal pressure increased until the gases penetrated the carbon layer and broken bubbles formed, as shown in the last SEM image of Fig. 6. The defects on the surfaces of the residual char reduced the stability of the carbon layer, which led to the decrease of flame retardancy.

In Fig. 7, there were two sets of fitting peaks located at  $1370\text{ cm}^{-1}$  and  $1610\text{ cm}^{-1}$  in the Raman spectrum of the residual char, corresponding to D band and G band, respectively. To our best knowledge, the D band corresponds to the vibration of carbon atoms in disordered graphite microstructure, while the G band corresponds to the vibration

of carbon atoms in the ordered structure [45–47]. The integrated intensity ratio ( $I_D/I_G$ ) of the two bands is used to measure the graphitization degree of residual carbon structure [10]. A smaller value represents a decrease in the disorder structure, which means the degree of graphitization is higher [48]. It's apparent that the  $I_D/I_G$  value of EP/10%TAP was 2.03, which was lower than that of EP. The decrease of value confirmed that the addition of TAP made contributions to the improvement of the graphitization degree of the residual char. This phenomenon of structural ordering further improved the stability of residual char, thus providing a positive effect on enhancing the flame retardancy of the material.

FTIR spectroscopy was adopted to investigate the structure of char residues of the EP and EP/10%TAP samples and the corresponding curves were shown in Fig. 8. It can be obviously seen from the FTIR spectra of the two samples that there were distinct absorption peaks at  $1594\text{ cm}^{-1}$  assigned to the vibration of C=C in benzene ring, manifesting the generation of polyaromatic structure after combustion. In addition, some new characteristic absorption peaks appeared in the infrared spectrogram of char residues for EP/10%TAP system. The peaks at  $1509$  and  $1244\text{ cm}^{-1}$  were attributed to the vibrations of P–C and P=O bonds, respectively [49]. The characteristic absorption peaks of P–O–C and P–O–P were respectively located at  $1105$  and  $875\text{ cm}^{-1}$  [26]. The occurrence of these characteristic absorption peaks revealed that the EP/10%TAP sample formed phosphorus-containing carbonization layer after combustion, which was derived from the degradation of the DOPO group. During combustion, the decomposition of the DOPO group produced some phosphorus-containing compounds, which promoted the

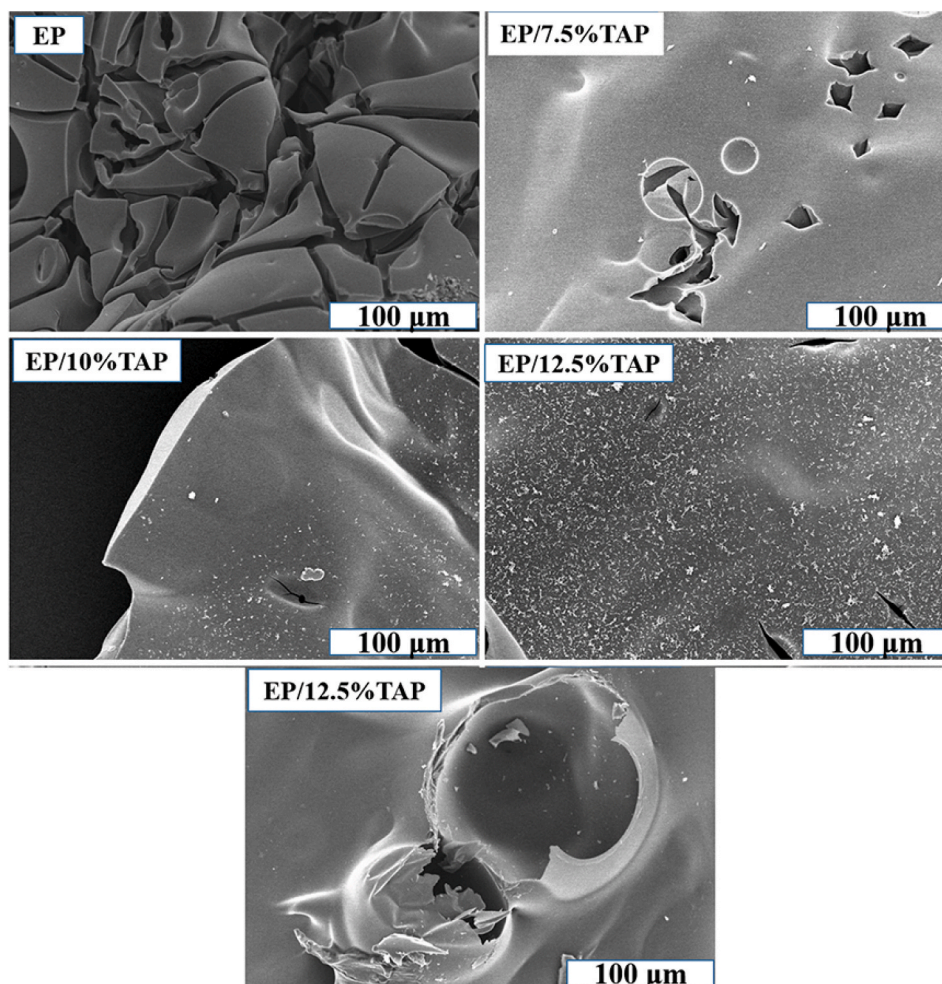


Fig. 6. SEM images of the char residues of epoxy thermosets.

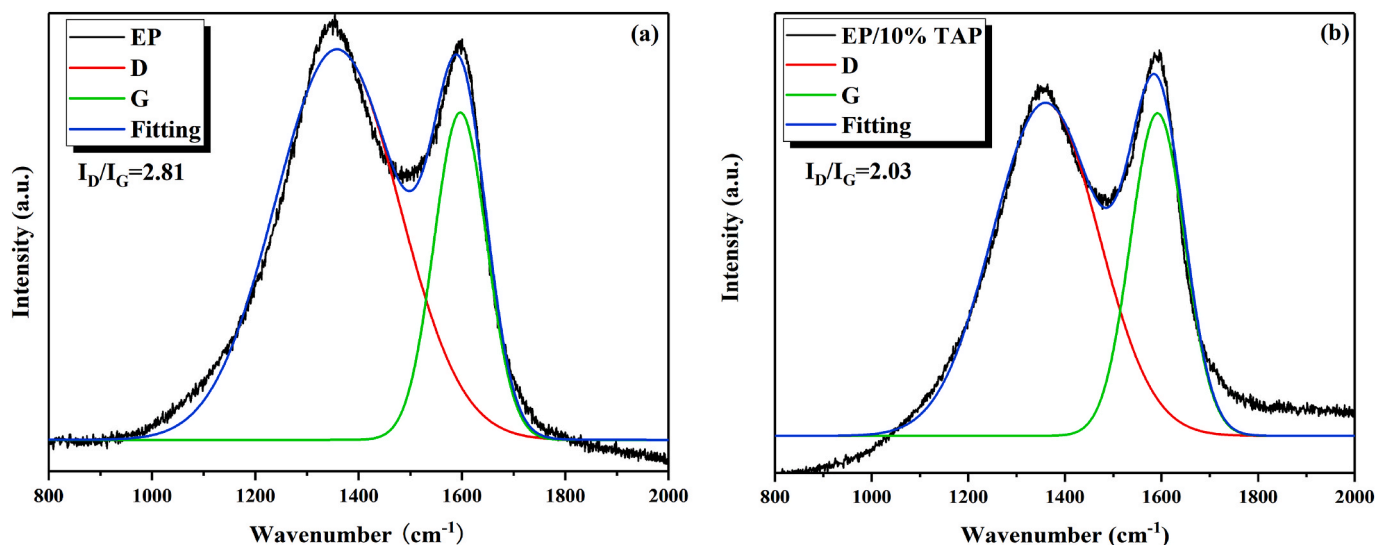


Fig. 7. Raman spectra of char residues for EP (a) and EP/10%TAP (b) after cone calorimeter tests.

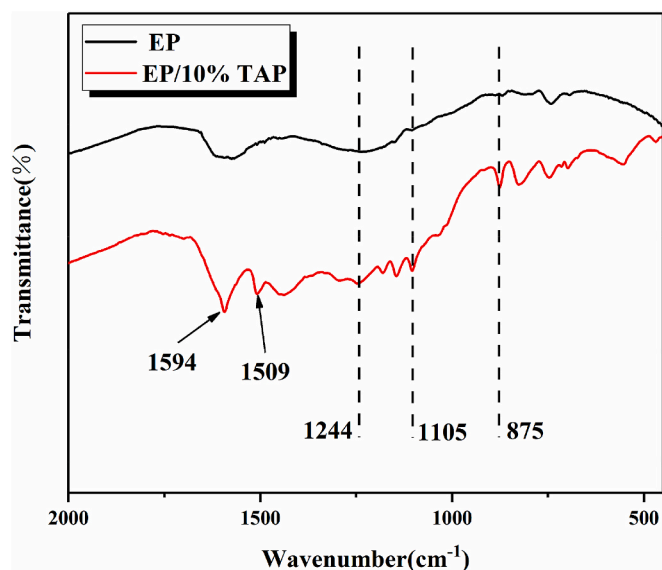


Fig. 8. FTIR spectra of char residues for EP and EP/10%TAP.

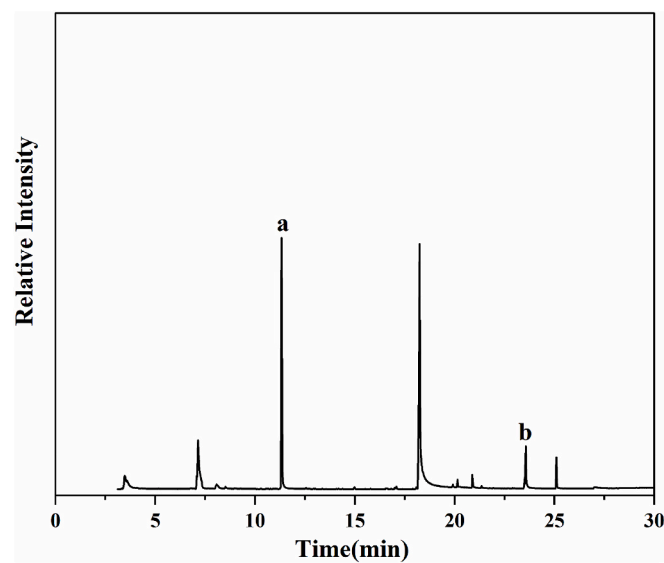


Fig. 9. Total ion chromatogram (TIC).

dehydration and carbonization of the matrix. The formation of a stable and continuous phosphorus-containing carbon layer can form a physical shielding layer to protect the substrate. Therefore, a good flame-retardant effect was exerted in the condensed phase.

### 3.5. Pyrolysis behavior

PY-GC/MS was utilized to study the pyrolysis behavior of TAP at 500 °C to further determine the gas-phase flame retardant model. Fig. 9 showed the total ion chromatogram (TIC) for the pyrolysis products of TAP. Two sets of MS spectra at different time points containing the characteristic peaks of a lot of typical fragment ions, were selected to analyze the pyrolysis products of TAP. The relevant results were shown in Fig. 10. The inferred pyrolysis route obtained from the characteristic peak analysis was presented in Scheme 2.

According to the synthetic process of TAP, we can know that TAP was synthesized from three raw materials. Similarly, the pyrolytic process of TAP was mainly the pyrolysis of these three materials. The first part was the pyrolysis of the theraldehyde fragment, which decomposes to

methylthiophene radical ( $m/z = 97$ ), thiophene ( $m/z = 84$ ). The second unit was the 2-benzothiazolamine fragment. The fragment at  $m/z = 150$  was related to 2-aminobenzothiazole. The decomposition products of benzothiazole ( $m/z = 135$ ) can be mainly classified as 2-aminothiophenol fragments ( $m/z = 124, 123$ ). Likewise, the fragments at  $m/z = 44$  and  $m/z = 108$  were regarded as the fragment of 2-aminobenzothiazole. Finally, the phosphaphenanthrene fragment was the third part, which decomposed into O=P-O-Ph radical ( $m/z = 139$ ) via the breaking of weak bonds, such as P-C. These fragments continued to decompose into  $\cdot\text{PO}_2$  radical ( $m/z = 63$ ).

As we all known, DOPO and its derivatives decompose to generate phosphorus-containing radicals during combustion. According to the previous analysis, the DOPO group contained in the flame retardant TAP also plays a corresponding role, which decomposes into  $\cdot\text{PO}_2$  radical during combustion to capture active radicals such as  $\cdot\text{H}$  and  $\cdot\text{OH}$  radicals, thus inhibiting burning and terminating the chain reaction [50]. Meanwhile, theraldehyde fragment and 2-aminobenzothiazole fragment were pyrolyzed to generate some inert radicals, which reacted with other radicals to obtain S/N-containing intermediates. In addition, according to the literature, it is reasonable to believe that the further

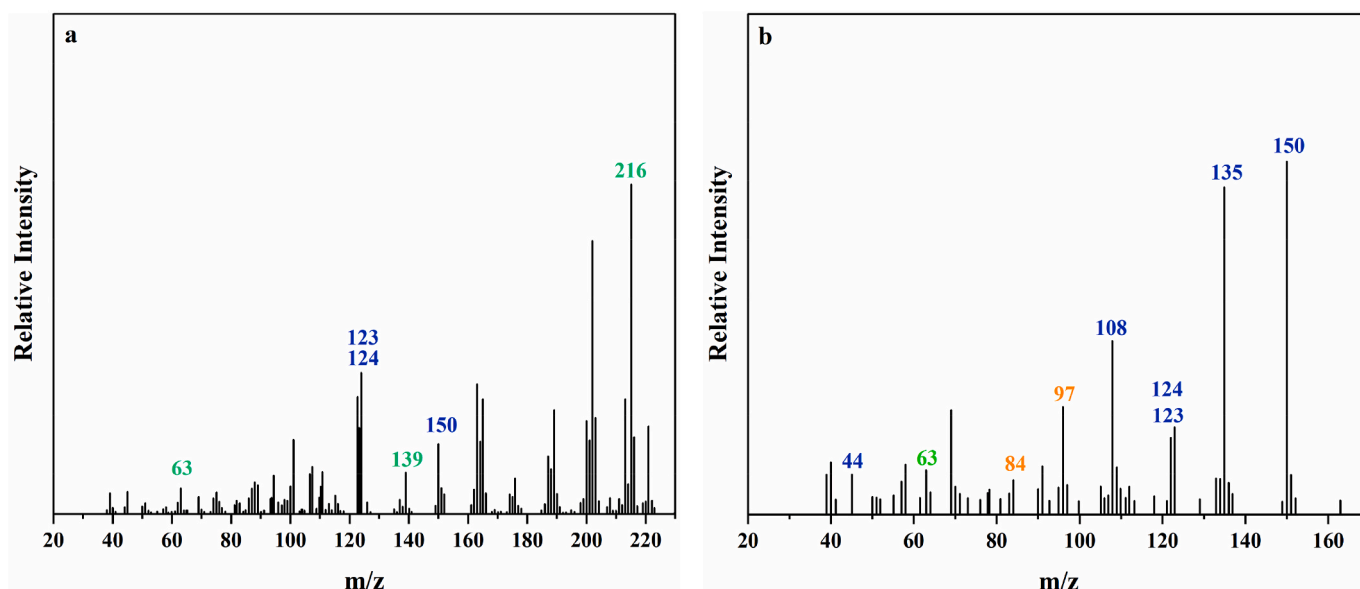
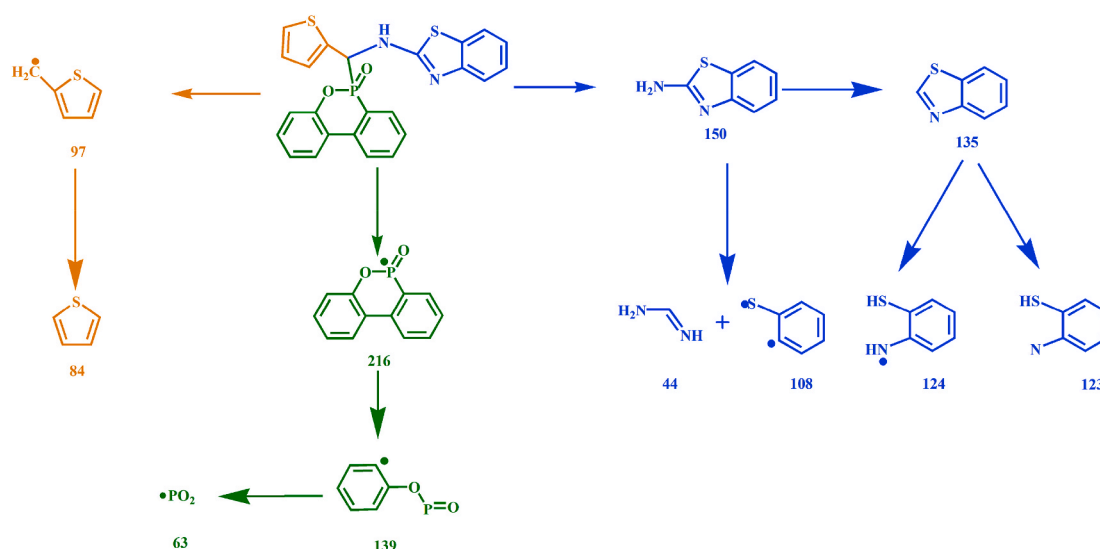


Fig. 10. MS spectra of main pyrolysis products of TAP.



Scheme 2. Proposed pyrolytic route of TAP.

disintegration of S/N-containing intermediates during combustion produced small molecules of nonflammable gas products, such as  $\text{SO}_2$  and  $\text{NH}_3$ , which can reduce oxygen concentration and combustion intensity [35,51]. Based on the above analysis, it is concluded that TAP endows EP with excellent gas-phase flame-retardant effect.

### 3.6. Proposed flame-retardant mechanism

According to the above-mentioned research results, it's confirmed that the addition of TAP endows the epoxy resin with excellent flame retardancy by exerting synergistic flame-retardant effect in the condensed phase and gas phase. Consequently, flame-retardant mechanism of TAP in EP was proposed and illustrated in Fig. 11.

In the process of combustion, TAP decomposes to produce some sulfur-containing and nitrogen-containing nonflammable gas products, diluting the combustible gases produced by the combustion of the substrate and the oxygen in the surrounding environment. It exerts dilution effect and reduces combustion intensity of gas phase. Besides, the decomposition of DOPO fragments result in the generation of

phosphorus-containing radicals, which combine with highly active radicals during combustion. Consequently, those radicals interrupt the combustion chain reaction and prevent the further combustion.

Simultaneously, some phosphorus-containing compounds produced in the condensed phase promote the formation of carbon and form a physical protective layer. With the generation of a large amount of gases, the carbon layer expands and internal structure of the residual char becomes complicated, which further restrains the exchange of oxygen and energy. It is the synergistic model that brings excellent flame-retardant properties to EP.

### 3.7. Heat resistance and mechanical properties

DMA was adopted to investigate the dynamic mechanical behavior of EP thermosets. The corresponding data and curves were shown in Table 5 and Fig. 12, respectively. Generally, the peak temperature in  $\tan \delta$  curve is identified as the glass transition temperature ( $T_g$ ) of the cured EP. It can be clearly seen in Fig. 12, the  $T_g$  value of the pure EP was 185 °C, while values of other samples decreased slightly on this basis. EP/

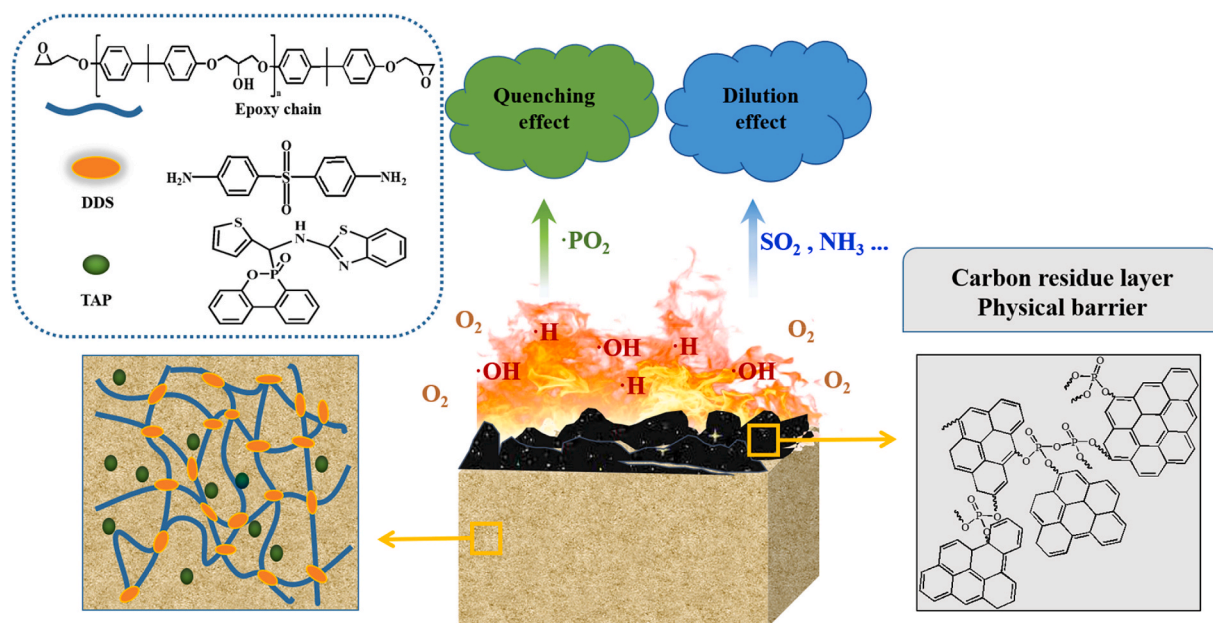


Fig. 11. Schematic diagram of the flame-retardant mechanism of TAP in EP.

12.5%TAP has the lowest  $T_g$  value of 177 °C, corresponding to a decrease of 4.3%. In order to explain this phenomenon, the crosslinking density ( $\nu_c$ ) was calculated according to the theoretical equation of rubber state with Eq. (1) [52], which was listed below.

$$\nu_c = E'/3RT \quad (1)$$

Where R represents the ideal gas constant (8.314 J/K·mol), T is the absolute temperature at  $T_g+40$  °C,  $E'$  is the storage modulus of the rubber plateau at  $T_g+40$  °C. The results obtained were listed in Table 5, where the crosslinking density decreased with the increase of the TAP addition amount. Although TAP contains several aromatic heterocycles, which is conducive to the improvement of  $T_g$ , the addition of the bulky molecule TAP results in a significant reduction in the cross-linking density (Table 5), which is the main factor for the decrease of  $T_g$ . Therefore, with the interaction of the two competing factors, macroscopic performance of the sample behaved a small decrease of  $T_g$ . Moreover, the storage modulus at 30 °C improved compared to pure EP, which is also due to the presence of rigid groups in the molecule. In summary, according to the slight decrease in  $T_g$  value of samples, it can be inferred that the thermosetting samples added with TAP have good heat-resistant property, which is of great significance for the practical application of EP.

As revealed in Fig. 13, flexural tests were used to evaluate the mechanical properties of samples. When the flame retardants were added to the resin matrix, the mechanical properties decreased as a whole, which was caused by the decline of the cross-linking density. However, as the dosage continued to increase, the flexural modulus of the sample gradually increased until it finally exceeded that of the pure epoxy resin. It may result from the fact that TAP contains heteroatoms (N, S) and it can form hydrogen bonds with the abundant hydroxyl groups in the

crosslinked network, whose presence can offset the mechanical deterioration caused by the decrease in crosslinking density [50,53]. Meanwhile, there are many aromatic rings in the structure, which may form additional  $\pi$ - $\pi$  interaction with matrix [38]. Therefore, the mechanical properties of the epoxy resin are not significantly deteriorated after the introduction of the flame retardant. It can be further concluded that flame-retardant epoxy resin samples maintained good mechanical properties.

#### 4. Conclusion

In this paper, a novel P/N/S-containing high-efficiency flame retardant (TAP) was designed and synthesized from DOPO and heterocyclic compounds containing sulfur and nitrogen elements. Although TGA revealed that the degradation temperature of epoxy resin decreased slightly, the degradation rate of the resin decreased and the fire safety were greatly improved. When the phosphorus content was only 0.48%, EP/7.5%TAP passed the vertical burning V-0 rating, while the LOI value dramatically increased from 22.8% to 30.8%. Furthermore, EP/10%TAP thermoset exhibited the lowest PHRR and THR values, which were respectively decreased by 41.26% and 35.70% compared with those of pure EP. In addition, the introduction of flame retardant endowed the substrate with smoke-suppression properties and improved the char residue. Subsequently, the analysis of the flame-retardant mechanism demonstrated that TAP can not only play a dilution and quenching effect in the gas phase, but also can promote the formation of a phosphorus-containing stable carbon layer. The presence of carbon layer acts as a physical shield, reducing the exchange efficiency of heat, combustibles, and oxygen with the substrate, thereby limiting the further burning of the material. After the introduction of TAP into the resin matrix,  $T_g$  of the samples only slightly decreased from 185 to 177 °C due to the decrease in crosslinking density, while the storage modulus increased because of the introduction of rigid groups. Besides, the decrease of crosslinking density and intermolecular interaction affected the mechanical properties of resin. In comparison with neat EP, EP/12.5%TAP exhibited better flexural modulus while the mechanical properties of other samples decreased slightly. Consequently, TAP can bring high-efficiency flame retardancy to the matrix and maintain satisfactory heat resistance and mechanical properties of the matrix, which exhibited a great application potential in the field of high-performance polymers and their composite materials.

Table 5

Thermomechanical properties of epoxy thermosets.

Sample	$T_g$ (°C)	Storage modulus at 30 °C (MPa)	Storage modulus at $T_g+40$ °C (MPa)	$\nu_c \times 10^{-3}$ (mol/m <sup>3</sup> )
EP	185	2926	47.29	3.81
EP/7.5%TAP	185	2966	38.94	3.13
EP/10%TAP	178	3200	32.95	2.69
EP/12.5%TAP	177	3141	31.59	2.59

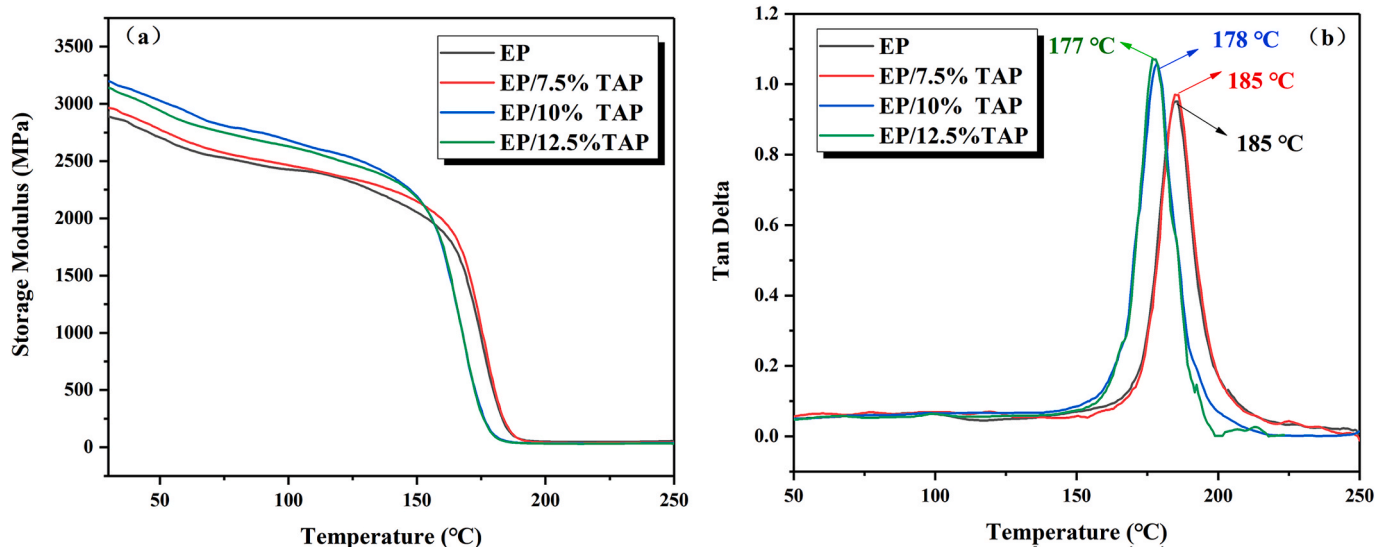


Fig. 12. DMA curves of epoxy thermostets.

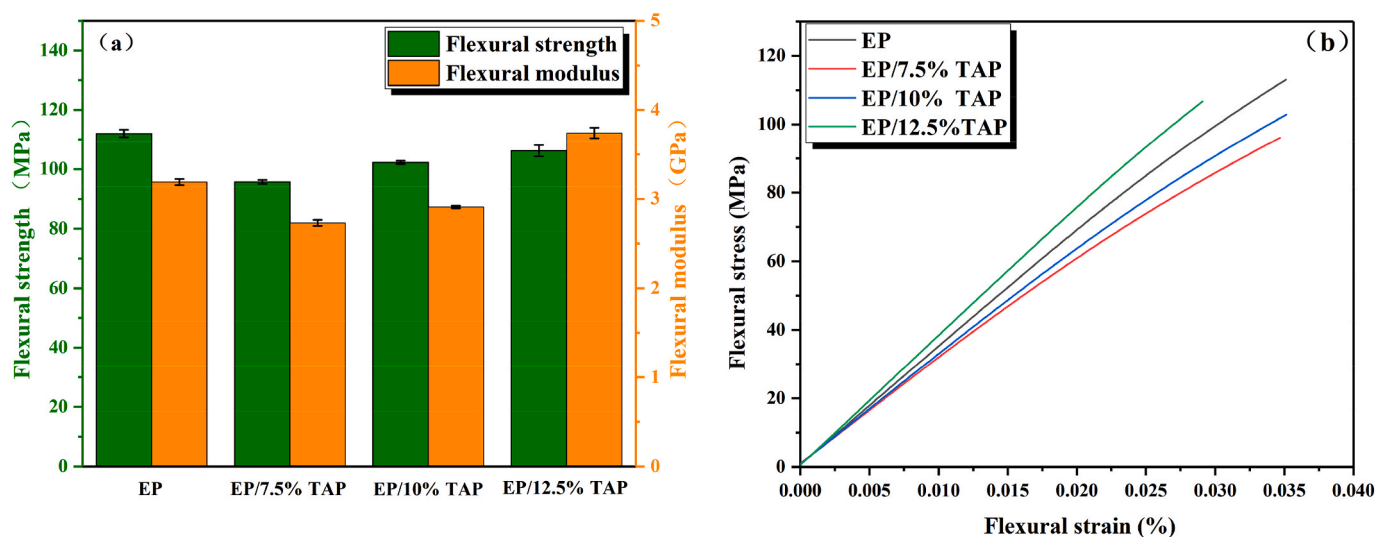


Fig. 13. Flexural strength as well as flexural modulus (a), and the stress-strain curves of all the EP samples (b).

#### CRediT authorship contribution statement

**Jiahao Zou:** Conceptualization, Investigation, Writing-original draft, Writing-review & editing. **Huajun Duan:** Conceptualization, Writing-review & editing, Supervision. **Yongsheng Chen:** Investigation, Writing-review & editing. **Sa Ji:** Writing-review & editing. **Jianfan Cao:** Investigation, Writing-review & editing. **Huiru Ma:** Supervision.

#### Declaration of competing interest

The authors declare that they have no known competing financial interests or personal relationships that could have appeared to influence the work reported in this paper.

#### Acknowledgments

This work was supported by the National Natural Science Foundation of China (51573144), the Natural Science Foundation of Hubei Province (ZRMS2019001284) and the Fundamental Research Funds for the Central Universities (WUT:2019III164CG).

#### References

- [1] Fang F, Ran S-Y, Fang Z-P, Song P-A, Wang H. Improved flame resistance and thermo-mechanical properties of epoxy resin nanocomposites from functionalized graphene oxide via self-assembly in water. *Compos B Eng* 2019;165:406–16.
- [2] Chen R, Hu K, Tang H, Wang J, Zhu F, Zhou H. A novel flame retardant derived from DOPO and piperazine and its application in epoxy resin: flame retardance, thermal stability and pyrolysis behavior. *Polym Degrad Stabil* 2019;166:334–43.
- [3] Xue Y, Shen M, Zeng S, Zhang W, Hao L, Yang L, Song P. A novel strategy for enhancing the flame resistance, dynamic mechanical and the thermal degradation properties of epoxy nanocomposites. *Mater Res Express* 2019;6(12):125003.
- [4] Liu L, Xu Y, Xu M, Li Z, Hu Y, Li B. Economical and facile synthesis of a highly efficient flame retardant for simultaneous improvement of fire retardancy, smoke suppression and moisture resistance of epoxy resins. *Compos B Eng* 2019;167:422–33.
- [5] Zhang K, Han M, Han L, Ishida H. Resveratrol-based tri-functional benzoxazines: synthesis, characterization, polymerization, and thermal and flame retardant properties. *Eur Polym J* 2019;116:526–33.
- [6] Huo S, Yang S, Wang J, Cheng J, Zhang Q, Hu Y, et al. A liquid phosphorus-containing imidazole derivative as flame-retardant curing agent for epoxy resin with enhanced thermal latency, mechanical, and flame-retardant performances. *J Hazard Mater* 2020;386:121984.
- [7] Pourchet S, Sonnier R, Ben-Abdelkader M, Gaillard Y, Ruiz Q, Placet V, et al. New reactive isoeugenol based phosphate flame retardant: toward green epoxy resins. *ACS Sustainable Chem Eng* 2019;7(16):14074–88.

- [8] Fang F, Huo S, Shen H, Ran S, Wang H, Song P, Fang Z. A bio-based ionic complex with different oxidation states of phosphorus for reducing flammability and smoke release of epoxy resins. *Compos Commun* ;17:104–8.
- [9] Fang F, Song P, Ran S, Guo Z, Wang H, Fang Z. A facile way to prepare phosphorus-nitrogen-functionalized graphene oxide for enhancing the flame retardancy of epoxy resin. *Compos Commun* 2018;10:97–102.
- [10] Yu B, Xing W, Guo W, Qiu S, Wang X, Lo S, et al. Thermal exfoliation of hexagonal boron nitride for effective enhancements on thermal stability, flame retardancy and smoke suppression of epoxy resin nanocomposites via sol-gel process. *J Mater Chem A* 2016;4(19):7330–40.
- [11] Howell BA, Lienhart GW, Livingstone VJ, Aulakh D. 1-Dopyl-1,2-(4-hydroxyphenyl) ethene: a flame retardant hardener for epoxy resin. *Polym Degrad Stabil* 2020;175:109110.
- [12] Liu S, Yu B, Feng Y, Yang Z, Yin B. Synthesis of a multifunctional bisphosphate and its flame retardant application in epoxy resin. *Polym Degrad Stabil* 2019;165:92–100.
- [13] Ma C, Qiu S, Wang J, Sheng H, Zhang Y, Hu W, et al. Facile synthesis of a novel hyperbranched poly (urethane-phosphine oxide) as an effective modifier for epoxy resin. *Polym Degrad Stabil* 2018;154:157–69.
- [14] Kim YO, Cho J, Yeo H, et al. Flame retardant epoxy derived from tannic acid as bio-based hardener. *ACS Sustainable Chem Eng* 2019;7(4):3858–65.
- [15] Balabanovich AI, Hornung A, Merz D, et al. The effect of a curing agent on the thermal degradation of fire retardant brominated epoxy resins. *Polym Degrad Stabil* 2004;85(1):713–23.
- [16] Howell BA, Han X. Effective bio-based phosphorus flame retardants from starch-derived bis-2,5-(hydroxymethyl)furan. *Molecules* 2020;25:592.
- [17] Wu H, Hu R, Zeng B, Yang L, Chen T, Zheng W, et al. Synthesis and application of aminophenyl-s-triazine derivatives as potential flame retardants in the modification of epoxy resins. *RSC Adv* 2018;8(66):37631–42.
- [18] Schmidt C, Ciesielski M, Greiner L, Döring M. Novel organophosphorus flame retardants and their synergistic application in novolac epoxy resin. *Polym Degrad Stabil* 2018;158:190–201.
- [19] Howell BA, Alrubayyi A. 2-Dopyl-1,4-di(2-dopylpropanoyl) benzene, an effective phosphorus flame retardant. *Polym Degrad Stabil* 2019;162:196–200.
- [20] Qiu Y, Liu Z, Qian L, Hao J. Pyrolysis and flame retardant behavior of a novel compound with multiple phosphaphenanthrene groups in epoxy thermosets. *J Anal Appl Pyrol* 2017;127:23–30.
- [21] Zhao J, Dong X, Huang S, Tian X, Song L, Yu Q, et al. Performance comparison of flame retardant epoxy resins modified by DPO-PHE and DOPO-PHE. *Polym Degrad Stabil* 2018;156:89–99.
- [22] Wu H, Li Y, Zeng B, Chen G, Wu Y, Chen T, et al. A high synergistic P/N/Si-containing additive with dandelion-shaped structure deriving from self-assembly for enhancing thermal and flame retardant property of epoxy resins. *React Funct Polym* 2018;131:89–99.
- [23] Carja ID, Serbezeanu D, Vlad-Bubulac T, et al. A straightforward, eco-friendly and cost-effective approach towards flame retardant epoxy resins. *J Mater Chem A* 2014;2(38):16230–41.
- [24] Mu X, Wang D, Pan Y, Cai W, Song L, Hu Y. A facile approach to prepare phosphorus and nitrogen containing macromolecular covalent organic nanosheets for enhancing flame retardancy and mechanical property of epoxy resin. *Compos B Eng* 2019;164:390–9.
- [25] Zhou J, Heng Z, Zhang H, Chen Y, Zou H, Liang M. High residue bio-based structural-functional integration epoxy and intrinsic flame retardant mechanism study. *RSC Adv* 2019;9(71):41603–15.
- [26] Huo S, Wang J, Yang S, Li C, Wang X, Cai H. Synthesis of a DOPO-containing imidazole curing agent and its application in reactive flame retarded epoxy resin. *Polym Degrad Stabil* 2019;159:79–89.
- [27] Jian R-K, Ai Y-F, Xia L, Zhang Z-P, Wang D-Y. Organophosphorus heteroaromatic compound towards mechanically reinforced and low-flammability epoxy resin. *Compos B Eng* 2019;168:458–66.
- [28] Wang P, Chen L, Xiao H, Zhan T. Nitrogen/sulfur-containing DOPO based oligomer for highly efficient flame-retardant epoxy resin. *Polym Degrad Stabil* 2020;171:109023.
- [29] Ye X, Li J, Zhang W, Yang R, Li J. Fabrication of eco-friendly and multifunctional sodium-containing polyhedral oligomeric silsesquioxane and its flame retardancy on epoxy resin. *Compos B Eng* 2020;191:107961.
- [30] Qiu Y, Qian L, Chen Y, Hao J. Improving the fracture toughness and flame retardant properties of epoxy thermosets by phosphaphenanthrene/siloxane cluster-like molecules with multiple reactive groups. *Compos B Eng* 2019;178:107481.
- [31] Qiu S, Hou Y, Xing W, et al. Self-assembled supermolecular aggregate supported on boron nitride nanoplatelets for flame retardant and friction application. *Chem Eng J* 2018;349:223–34.
- [32] Tang H, Zhou H. A novel nitrogen, phosphorus, and boron ionic pair compound toward fire safety and mechanical enhancement effect for epoxy resin. *Polym Adv Technol* 2020;31:885–97.
- [33] Xu M, Zhao W, Li B, et al. Synthesis of a phosphorus and sulfur-containing aromatic diamine curing agent and its application in flame retarded epoxy resins. *Fire Mater* 2015;39:518–32.
- [34] Cheng J, Wang J, Yang S, Zhang Q, et al. Aminobenzothiazole-substituted cyclotriphosphazene derivative as reactive flame retardant for epoxy resin. *React Funct Polym* 2020;146:104412.
- [35] Wang P, Xia L, Jian R, et al. Flame-retarding epoxy resin with an efficient P/N/S-containing flame retardant: preparation, thermal stability, and flame retardance. *Polym Degrad Stabil* 2018;149:69–77.
- [36] Jin S, Qian L, Qiu Y, Chen Y, Xin F. High-efficiency flame retardant behavior of bi-DOPO compound with hydroxyl group on epoxy resin. *Polym Degrad Stabil* 2019;166:344–52.
- [37] Liu C, Chen T, Yuan CH, Song CF, Chang Y, Chen GR, et al. Modification of epoxy resin through the self-assembly of a surfactant-like multi-element flame retardant. *J Mater Chem* 2016;4(9):3462–70.
- [38] Wang P, Xiao H, Duan C, Wen B, Li Z. Sulfathiazole derivative with phosphaphenanthrene group: synthesis, characterization and its high flame-retardant activity on epoxy resin. *Polym Degrad Stabil* 2020;173:109078.
- [39] Jian R, Wang P, Xia L, Zheng X. Effect of a novel P/N/S-containing reactive flame retardant on curing behavior, thermal and flame-retardant properties of epoxy resin. *J Anal Appl Pyrol* 2017;127:360–8.
- [40] Zhang Q, Yang S, Wang J, et al. A DOPO based reactive flame retardant constructed by multiple heteroaromatic groups and its application on epoxy resin: curing behavior, thermal degradation and flame retardancy. *Polym Degrad Stabil* 2019;167:10–20.
- [41] Chu F, Ma C, Zhang T, et al. Renewable vanillin-based flame retardant toughening agent with ultra-low phosphorus loading for the fabrication of high-performance epoxy thermoset. *Compos B Eng* 2020;190:107925.
- [42] Li Z, Gonzalez AJ, Heeralal VB, Wang D-Y. Covalent assembly of MCM-41 nanospheres on graphene oxide for improving fire retardancy and mechanical property of epoxy resin. *Compos B Eng* 2018;138:101–12.
- [43] Zhang Q, Wang J, Yang S, Cheng J, Ding G, Huo S. Facile construction of one-component intrinsic flame-retardant epoxy resin system with fast curing ability using imidazole-blocked bismaleimide. *Compos B Eng* 2019;177:107380–9.
- [44] Wu Q, Zhang Q, Zhao L, Li S-N, Wu L-B, Jiang J-X, et al. A novel and facile strategy for highly flame retardant polymer foam composite materials: transforming silicone resin coating into silica self-extinguishing layer. *J Hazard Mater* 2017;336:222–31.
- [45] Yang G, Wu WH, Wang YH, Jiao YH, Lu LY, Qu HQ, et al. Synthesis of a novel phosphazene-based flame retardant with active amine groups and its application in reducing the fire hazard of Epoxy Resin. *J Hazard Mater* 2019;366:78–87.
- [46] Wu J-N, Chen L, Fu T, Zhao H-B, Guo D-M, Wang X-L, et al. New application for aromatic Schiff base: high efficient flame-retardant and anti-dripping action for polyesters. *Chem Eng J* 2018;336:622–32.
- [47] Jian RK, Ai YF, Xia L, Zhao LJ, Zhao HB. Single component phosphamide-based intumescent flame retardant with potential reactivity towards low flammability and smoke epoxy resins. *J Hazard Mater* 2019;371:529–39.
- [48] Yu B, Shi Y, Yuan B, Qiu S, Xing W, Hu W, Song L, Lo S, Hu Y. Enhanced thermal and flame retardant properties of flame-retardant-wrapped graphene/epoxy resin nanocomposites. *J Mater Chem A* 2015;3:8034–44.
- [49] Li Z, Chen M, Li S, Fan X, Liu C. Simultaneously improving the thermal, flame-retardant and mechanical properties of epoxy resins modified by a novel multi-element synergistic flame retardant. *Macromol Mater Eng* 2019;304(4):1800619.
- [50] Duan H, Chen Y, Ji S, Hu R, Ma H. A novel phosphorus/nitrogen-containing polycarboxylic acid endowing epoxy resin with excellent flame retardance and mechanical properties. *Chem Eng J* 2019;375.
- [51] Jian R, Wang P, Duan W, Wang J, Zheng X, Weng J. Synthesis of a novel P/N/S-containing flame retardant and its application in epoxy resin: thermal property, flame retardance, and pyrolysis behavior. *Ind Eng Chem* 2016;55(44):11520–7.
- [52] Cheng J, Wang J, Yang S, Zhang Q, Huo S, Zhang Q, et al. Benzimidazolyl-substituted cyclotriphosphazene derivative as latent flame-retardant curing agent for one-component epoxy resin system with excellent comprehensive performance. *Compos B Eng* 2019;177:10744–107450.
- [53] Shao Z-B, Zhang M-X, Li Y, Han Y, Ren L, Deng C. A novel multi-functional polymeric curing agent: synthesis, characterization, and its epoxy resin with simultaneous excellent flame retardance and transparency. *Chem Eng J* 2018;345:471–82.